

**How to Cite:**

Abbas, S. M., & Kadam, Z. M. (2022). A new method preparation and spectroscopic characterization of the nano organic reagent derivatives from pyrogallol and its complex with iron (III). *International Journal of Health Sciences*, 6(S4), 5890–5899.  
<https://doi.org/10.53730/ijhs.v6nS4.9464>

## **A new method preparation and spectroscopic characterization of the nano organic reagent derivatives from pyrogallol and its complex with iron (III)**

**Shatha M. Abbas**

Department of chemistry, college of science, University of Al-Qadisiyah, Diwaniyah, Iraq

**Zeina M. Kadam**

Department of chemistry, college of science, University of Al-Qadisiyah, Diwaniyah, Iraq  
Corresponding author email: [dr.zeinakadam@gmail.com](mailto:dr.zeinakadam@gmail.com)

**Abstract**---In this research, the nanoorganic reagent 4 (4-sulphophenylazo) pyrogallol was prepared by the method of forming diazonium salt in an acidic medium by coupling the compound sulfadiazine with the compound pyrogallol. The reagent complex with iron (III) was also prepared. The prepared reagent and complex were diagnosed through electronic spectrometers, UV-Visible Spectrophotometers, IR, and X-ray diffraction measurements, XRD, and <sup>1</sup>H-NMR-C<sup>13</sup>-NMR measurements. The effect of the solvent, the acidity function, and the metal ratio of the 4-SPAP reagent were also studied, and the solid metal complex of iron was prepared from the transitional elements depending on the optimal conditions of concentration and molar ratio at the pH of this metal. The calibration curve of the iron complex was determined. Where the detection limit (LOD) was 2.2 ppm and the quantitative limit (LOQ) was 7.4 ppm.

**Keywords**---azo reagent, sulfadiazine, pyrogallol, spectral study.

### **Introduction**

Nanomaterials are considered one of the distinguished categories of very small materials that are prepared in the laboratory, or those that actually exist in nature and whose internal dimensions range between 1 and 100 nm. The purpose of minimizing the sizes of these materials is to make them behave differently from traditional large-sized materials whose dimensions are more than (100 nano) as

they have distinctive qualities and properties that are not found collectively in those traditional materials. This facilitates the delivery of medicines and therapeutic drugs to the affected part through membranes and vessels <sup>(1,2,3)</sup>. One of the important organic compounds that are used as reagents in the inorganic analysis of metal ions is the widespread azo compounds because of their ability to coordinate with most elements of the periodic table and their formation of stable and colored products <sup>(4,5)</sup>. This type of reagent contains the azo bridge group (-N=N-) <sup>(6,7,8)</sup>. The azo compounds are either aromatic or nitrogenous and are the most stable due to the presence of the phenomenon of resonance in them, as well as the speed of their interaction with metal ions, and the stability of the complexes that form. This is the reason for the wide spread of these kinds of azo compounds. As for aliphatic reagents, they are less widespread, and this is because of their rapid dissociation into nitrogen and hydrocarbons <sup>(9)</sup>.

## Methods

### Synthesis of 4(4-Sulphophenylazo)pyrogallol

The reagent (4-SPAP) was prepared according to the standard azo method<sup>(10)</sup>, where 0.01 mol (2.27 g) of sulfadiazine was dissolved in a mixture of 10 ml of HCL 37% and 80 ml of distilled water, and the mixture was cooled to a temperature of 5 - 0 C). Then add 0.01 mol of sodium nitrite and cool for a period of 30 minutes. Then this diazonium chloride solution was added to a solution of (1.26 g) 0.01 mol of pyrogallol dissolved in a mixture of 30 ml of ethanol and 100 ml of NaOH, leaving the mixture for two hours at a temperature of (5 - 0 C). Then add 100 ml of distilled water and leave the mixture for 24 hours. Then the precipitate was filtered and washed several times with ion-free water and recrystallized with absolute ethanol, and the precipitate was left to dry. the melting point (167-165 C).

### Preparation of solutions

The standard solution of organic reagent: The reagent solution was prepared by dissolving 0.1935 gm (0.01M) of the reagent (4-SPAP) in 50 ml of ethanol. Standard solution of organic reagent complexes: (0.01M) 0.081gm of FeCl<sub>3</sub> metal salt is dissolved in 50ml of buffer solution at pH = 7 to perform the spectroscopic measurement of the standard iron experiment .

Study the effect of solvent: Studying the effect of a change on the 4-SPAP reagent, different polar solvents were used, such as ethanol, methanol, toluene, 2-propanol ethylene glycol, THF, DMSO, and acetone in the laboratory, and by dissolving a certain weight of the reagent in the solvent used Then, using the UV-Vis device, determine the change in molar absorption and the maximum wavelength.

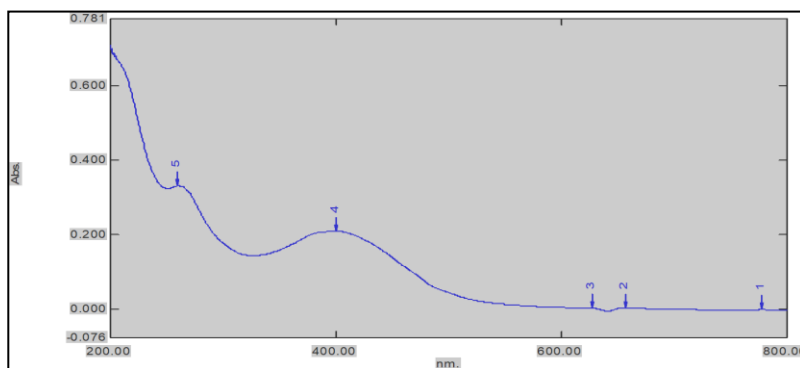
Study of the effect ( pH): The effect of the pH function of each metal complex under study was studied with a fixed concentration within the range (1.25\*10<sup>-4</sup> - 2.5\*10<sup>-4</sup>) M.

Iron complex (III) preparation) Fe(4-SPAP) 2: The iron complex was prepared with a molar ratio of L:M [2:1] by adding 0.02 mol of reagent dissolved in 30 ml of ethanol to 0.01 mol of iron chloride (III) dissolved in 30 ml of buffer solution at pH = 9. The color changed at the moment of mixing to a reddish brown. After that, the mixture was heated for 30 minutes at a temperature of 60°C, and the formation of a black precipitate was observed.

## Results and discussion

### Spectral study

Spectrum of UV-Vis Absorption Figure (1): The bands of the absorption spectrum of ultraviolet visible rays of the prepared reagent show two transitions, the first band due to the transitions from ( $n \rightarrow \pi^*$ ) to the azo group, and the second band goes back to the electronic transition ( $\pi \rightarrow \pi^*$ ) goes back to the electronic transition ( $\pi \rightarrow \pi^*$ ). And figure (2) shows the UV spectra of the iron complex.



Figure( 1) UV-Visible Spectrum Detector(4- SPAP) at max=400nm

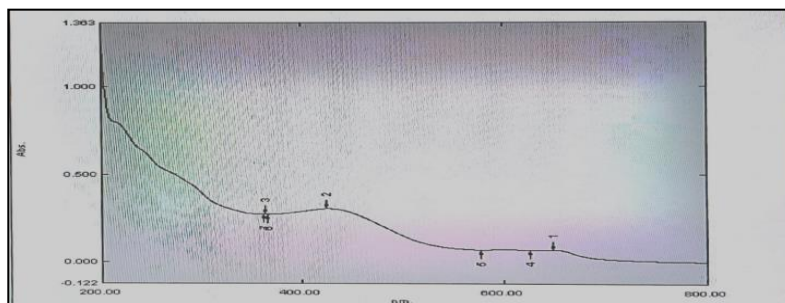


Figure (2) UV-visible spectrum of Fe(III) complex at max=425nm

Infrared absorption spectrum: The prepared reagent was described by their spectrum of FT-IR, as shown in Figure (3,4). Table (1) shows the sites of the beams of the reagent, and iron complex. Table (1) shows the important beams in the infrared spectra of the (4-SPAP) detector and the iron complex in unit ( $\text{cm}^{-1}$ ).

Compound	SPA P 4-	Fe(SPAP) <sub>2</sub>
u(N-H) amine	3348.54 $\text{cm}^{-1}$	3632.08 $\text{cm}^{-1}$

$\nu(\text{O-H})$ Ar	3342.75 $\text{cm}^{-1}$	3412.19 $\text{cm}^{-1}$
$\nu(\text{C-H})$ Ar.	3053.42 $\text{cm}^{-1}$	3144.07 $\text{cm}^{-1}$
$\nu(\text{N=N})$	1438.94 $\text{cm}^{-1}$	1437.02 $\text{cm}^{-1}$
$\nu(\text{C=C})$	1581.68 $\text{cm}^{-1}$	1581.68 $\text{cm}^{-1}$
SO <sub>2</sub> group	1340.57 $\text{cm}^{-1}$ <sup>1</sup> asym	1340.57 $\text{cm}^{-1}$ asym
	1151.54 $\text{cm}^{-1}$ sym	1155.40 $\text{cm}^{-1}$ <sup>1</sup> sym
$\nu(\text{M-O})$	-----	478.36-420.50 $\text{cm}^{-1}$
$\nu(\text{M-N})$	-----	511.15 $\text{cm}^{-1}$

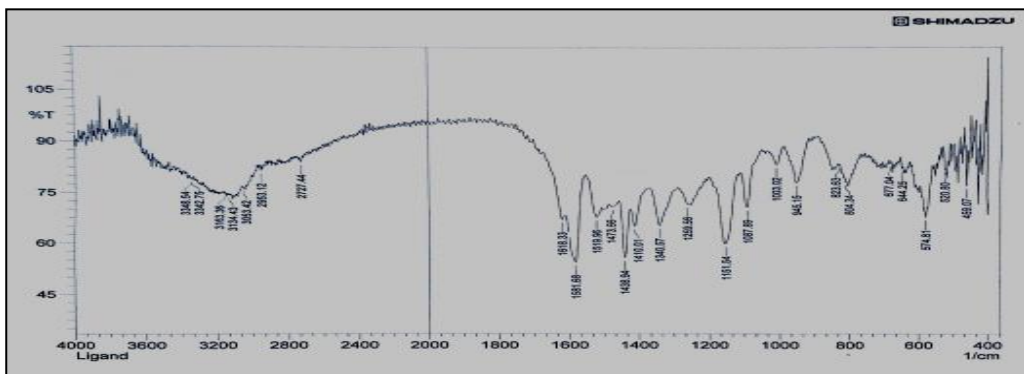


Figure (3) shows the FT-IR spectrum of the (4-SPAP) detector.

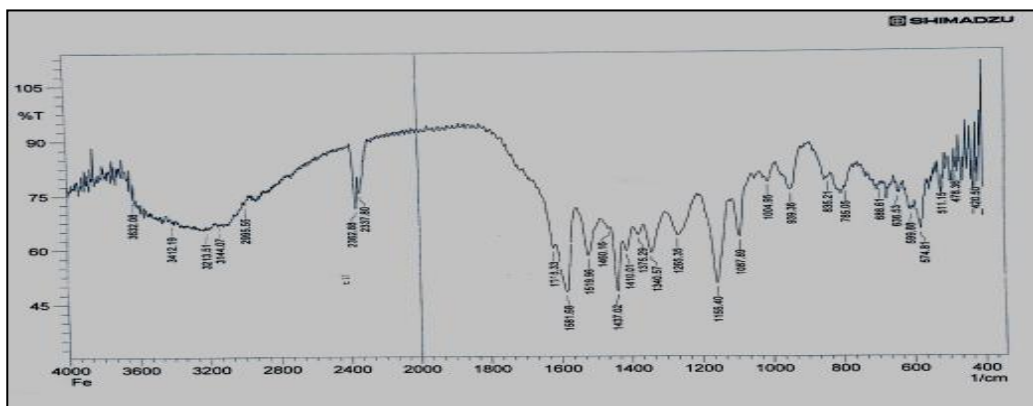


Figure (4) shows the FT-IR spectrum of the Fe(SPAP)<sub>2</sub> complex.

(4-SPAP) reagent and iron complex H1-NMR-C13-NMR spectrophotometer <sup>1</sup>H-NMR : was diagnosed by (4-SPAP) reagent using the solvent (DMSO-d<sub>6</sub>). An A band appeared at = 15.3 ppm, which represents the most acidic OH group of the pyrogallol ring. As for the group (1H-SO<sub>2</sub>NH) at = 11.5 ppm, as well as the protons of the ring, pyridine and the benzene ring in sulfadiazine at = 7.3-8.5 ppm, as for the proton attached to the nitrogen atom in the azo group (N=N) on one side of the pyrogallol ring and the benzene ring on the other side of the azo group, the band appears at 6.5-7 ppm. A single wide beam belonging to the water molecule was observed at = 3.5ppm and the solvent bundle of DMSO at = 2.5ppm,

as shown in Figure (5). As for the spectrum of the  $C^{13}$ -NMR detector (4-SPAP) using the solvent DMSO, it was observed that a signal appeared at the sites (116.19, 158.81, 157.41 ppm) back (C = C) of the pyridine ring. As for the benzene ring, it shows the sign (C = C) at the sites (121.98, 127.89, 129.33, 129.43 ppm), as well as the appearance of At (133.33, 140.96, 146.41 ppm), but the solvent signal appeared at the site. (40) ppm, as shown in Figure (6).

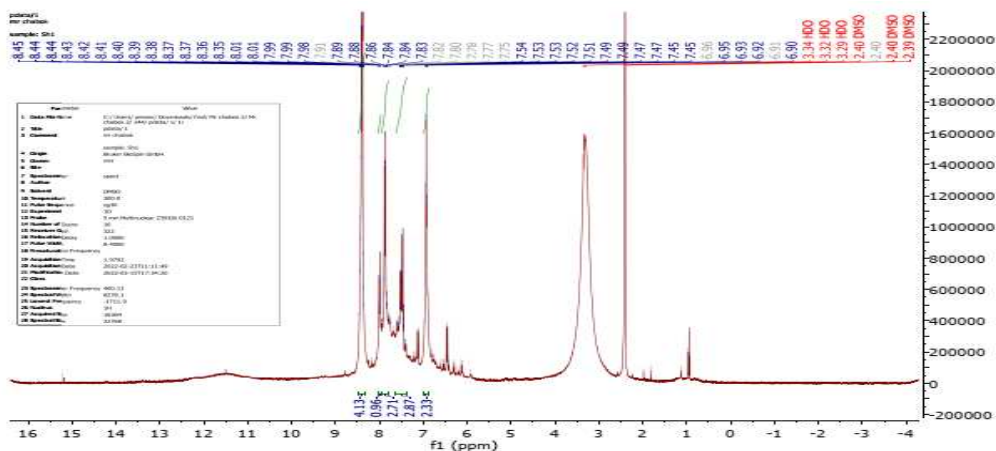


Figure (5):  $^1H$ -NMR spectrum of a (4-SPAP) detector

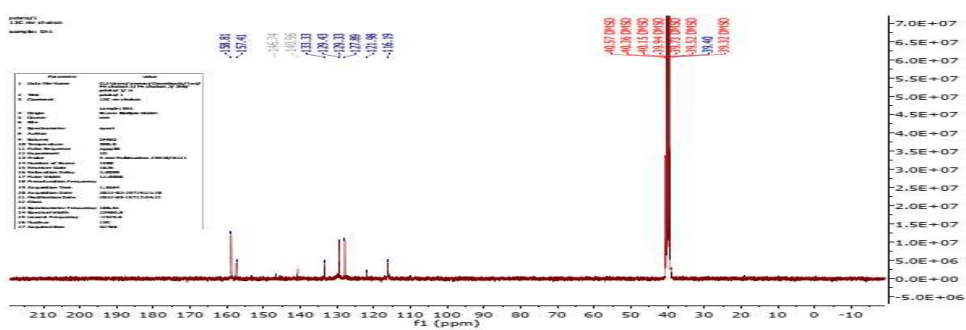


Figure (6):  $C^{13}$ -NMR spectrum of the (4-SPAP) detector.

**X-Ray Diffraction (XRD):** To study the crystal structures of each of the reagent and the iron complex in its solid state, we use X-ray diffraction. The spectra are shown in Table (2) and Figure (9) within the angular range  $2\theta$  (20- 80) to know some of their structural properties such as crystal structure, crystal size, and its purity can be estimated. The diffraction peaks have a review of several things (11,12). The appearance of high peaks for the prepared iron reagent and complex is an indication on the presence of crystal levels and a crystal structure of high homogeneity high crystalline nature, while point peak Low crystalline X-ray spectroscopy on low crystalline structures<sup>13,14</sup>. The detector also showed several reflections and the highest intensity was (I/I0) 100% at  $2\theta = 31.8817^\circ$  corresponding to the value of  $d = 2.80704$ .

Table (2) represents the values of d-spacing, diffraction angles, relative intensity, and average crystal size of the reagent (4-SPAP) in its solid state

Material	$2\theta$	FWHM	Intensity (I/I <sub>0</sub> ) %	d-spacing (Å)	Crystallite Size D(nm)	Average Size D(nm)
4-SPAP	31.8817	0.2952	100	2.80704	2.80704	24.61786
	45.6225	0.246	57.4	1.98851	1.98851	
	56.6475	0.2952	13.91	1.6249	1.6249	
	66.3888	0.2952	5.03	1.40815	1.40815	
	75.4719	0.2952	9.71	1.25965	1.25965	

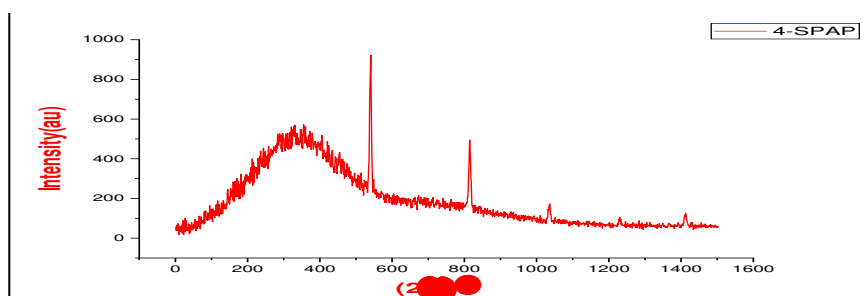
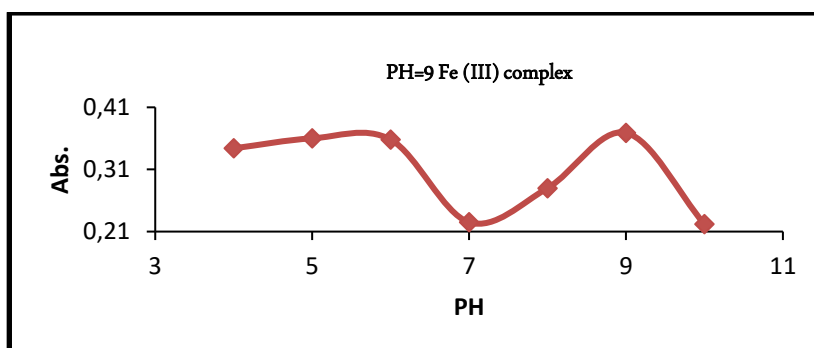


Figure (7): XRD spectrum of (4-SPAP) reagent

The effect of the acid function (pH): The appropriate pH of the iron ion was studied with the 4-SPAP reagent, and it had the highest absorbance at pH = 9, shown in figure (10):



Figure( 8) Effect of PH on absorbance at  $\lambda_{max}$  for Fe(III) mixing solutions with 4-SPAP

Study the effect of solvent: The aim of studying the effect of the solvent is to know the extent to which polarity affects the displacement of the absorption sites in the spectrum  $\lambda_{max}$ , As well as knowing the appropriate solvent for the process of

preparing the reagent and metal complexes during the study, as shown in the table (3):

Table (3) Effect of solvent on reagent 4 (4-SPAP) with concentration M ( $1 \times 10^{-4}$ ) in different solvents using an uv-visble spectrophotometer

protic solvents			aprotic solvents		
Solvent	Abs.	$\lambda_{\max}$	Solvent	Abs.	$\lambda_{\max}$
Ethanol	0.209	400	DMSO	0.167	269
Methanol	0.114	411	THF	0.274	402
2-propanol	0.063	409.5	Acetone	0.28	443
Ethylene glycol	0.194	409	Toluene	0.793	365

Molar ratio determines the ratio of( metal: ligand): The molar ratio is one of the important spectroscopic methods. This method is used to determine and specify the ratio of the metallic metal to the detector, to form the metal complex. As shown in the table (4):

Table (4): The molar absorbance of iron ion complex solutions with the azo reagent (4-SPAP) at the maximum wavelengths ( $\lambda_{\max} = 425\text{nm}$ ) corresponding to the molar ratios (M:L).

NO	M/L	Absorbance Fe(III)
1	1: 0.25	0.030
2	1: 0.5	0.036
3	1: 0.75	0.042
4	1: 1	0.055
5	1: 1.25	0.062
6	1: 1.5	0.073
7	1: 1.75	0.084
8	1: 2	0.096
9	1: 2.25	0.098
10	1: 2.5	0.102
11	1: 2.75	0.104
12	1: 3	0.106

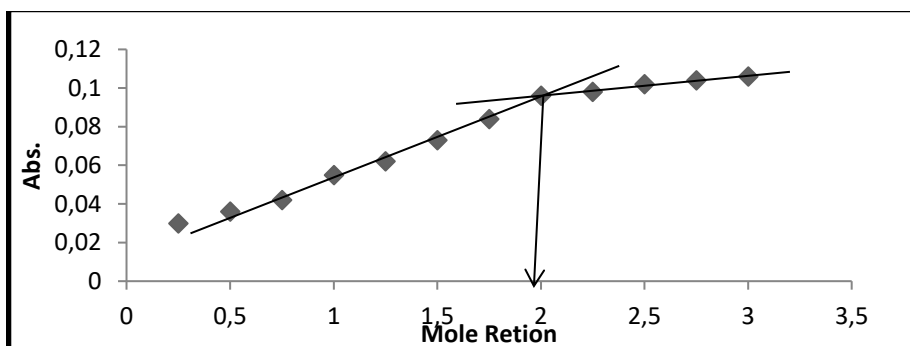


Figure (9): is a curve of the molar ratio of the iron complex with the reagent at 425 nm

Calibration Curve for Iron Complexes with Reagent 4-SPAP: The calibration curve for iron complexes was determined by preparing a series of standard solutions of iron complexes, respectively, using a (Visible-UV) device. Absorbance values for these solutions were obtained at their greatest wavelength. By plotting the absorbance values against concentration, the calibration curve was.

Table (5): Estimating the accuracy and validity of the analytical method for determining the concentration of iron ions

Parameter	Value(Fe <sup>3+</sup> )
$\lambda_{\max}$ nm	425
Arithmetic mean( $\bar{x}$ )	0.041889
standard deviation SD	0.0110277
simultaneous relative standard deviation %RSD	26.326176
Regression Equation	$Y=0.0149x-0.0163$
Limit of Detection (ppm)LOD	2.220351
Limit of Quantitation (ppm)LOQ	7.40117
Correlation Coefficient R <sup>2</sup>	0.977

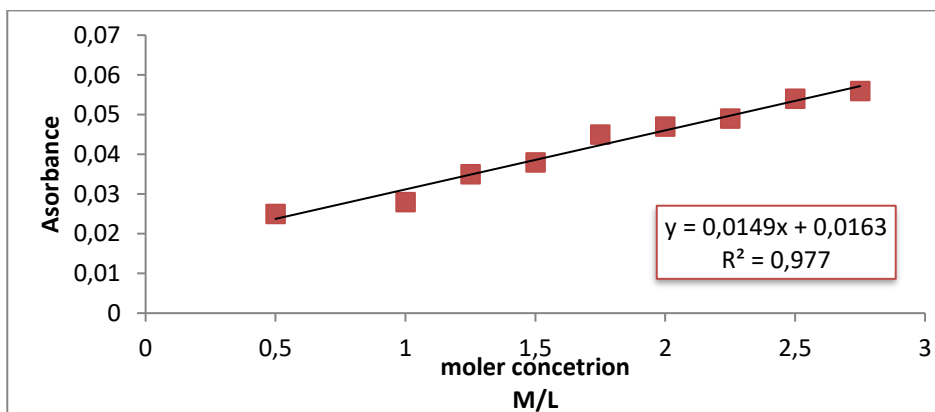


Figure (10): Calibration curve of the iron complex with the 4-SPAP detector at (425nm)

## Conclusion

A new nanoorganic reagent was prepared using the azo method by coupling sulfadiazine with pyrogallol as well as preparing the iron complex. The spectral properties were studied using the UV-Vis spectrum, where a peak appeared at the highest wavelength,  $\lambda_{\max} = 400\text{nm}$ , and the iron complex at  $\lambda_{\max} = 425\text{nm}$ , as well as IR and measured <sup>1</sup>H-NMR-C<sup>13</sup>-NMR as well as the crystal structure were revealed. For a detector with XRD technology, and from calculating the value of the particle size, it was found that it is within the nanoscale.

## References

1. Dr. Muhammad Sharif Al-Iskandarani, *Nanotechnology: For a Better Tomorrow*, Knowledge World Series, Kuwait, ISBN 978-99906-0-306-4, April 2010.
2. Dr. Ahmed Tawfiq Hijazi, *Nanotechnology: The New Technological Revolution*, House of Knowledge Treasures, Amman, Jordan, May 2011; ISBN 978-74-180-8.
3. D.Ata Hassen Darwish and Halla Hamid, Students' knowledge of nanotechnology application in the college of education at Gaza universities and their attitudes towards them.
4. Zeina Mohammed kadam, Raheem Abed Jeber, and Alaa Hussein Ali, *Azo Dyes on the Ligand (5-MeTAQ) Thin Films for Dye Sensitive Solar Cell Applications* Published under licence by IOP Publishing Ltd., *Journal of Physics: Conference Series*, Volume 1999, 2nd International Virtual Conference on Pure Science (2IVCPS 2021) 21–22 April 2021 (2IVCPS 2021) 21–22 April 2021.
5. Ali, A. H., Jwad, K., and Kadam, Z. M., Preparation and characterization of a novel ligand (5-MeTAQ) with Cd (II), Zn (II), and Hg (II) metal complexes. *IOP Conf. Series: Journal of Physics: Conf. Series*, 1294, (2019). 052039. 990
6. Nawras A. Alwan<sup>1</sup> and Zeina M. Kadam, Preparing and diagnosing the biological activity of some metallic complexes with the ligand 4-Benzophenol, Azopyrogallol(4), *IOP Conference Series: Earth and Environmental Science*, Volume 790, First International Virtual Conference on Environment and Natural Resources, March 24–25, 2021.
7. S.Keda, Y.Murakami, and K.Akatsuka, *Chem. Lett.*, vol. 363, 1981.
8. *Microchimica Acta*, 1 (1983), 75, M.Siroki and M.Koren.
9. H.Maradiya and V.Patel, *J. Serb. Chem. Soc.*, 66 (2001), 87.
10. Zainab A. Abid Alradaa and Zeina M. Kadam, Preparation, Characterization and Prevention 4-(4-Benzophenylazo) Pyrogallol and its Metal Complexes Cause Biological Pollution Published under licence by IOP Publishing Ltd., *IOP Conference Series: Earth and Environmental Science*, Volume 790, First International Virtual Conference on Environment & Natural Resources, 24–25 March 2021.
11. A. Masoudiasl, M. Montazerozohori, R. Naghiha, A. Assoud, P. McArdle, and M. S. Shalamzari, *Mater. Sci. and Eng. C*, 61, 809–823.
12. S. Bai, J. Hu, Li, R. Luo, A. J. *Mater. Chem.*, 21, (2011), 12288–12294.
13. V. S. Gavhane, A. S. Rajbhoj, and S. T. Gaikwad, *Der Pharma Chemica*, 8(2), (2016), 275-277.
14. Zainab A. Alradaa and Zeina M. Kadam, X-ray diffraction CHARACTERIZATION OF CRYSTAL STRUCTURE REGENT4 (4-Sulphophenyl Azo) Pyrogallol Published under licence by IOP Publishing Ltd., *Journal of Physics: Conference Series*, Volume 1999, 2nd International Virtual Conference on Pure Science (2IVCPS 2021), 21–22 April 2021.
15. Muthoharoh, B. L., Kartini, F., & Fitriahadi, E. (2022). Pregnant women's perceptions of anemia and iron supplement consumption. *International Journal of Health & Medical Sciences*, 5(2), 183-192. <https://doi.org/10.21744/ijhms.v5n2.1902>
16. Widana, I.K., Sumetri, N.W., Sutapa, I.K., Suryasa, W. (2021). Anthropometric measures for better cardiovascular and musculoskeletal

health. *Computer Applications in Engineering Education*, 29(3), 550–561.  
<https://doi.org/10.1002/cae.22202>